*International Journal of Engineering & Technology*, 7 (4.8) (2018) 130-138

International Journal of Engineering & Technology

*Website:www.sciencepubco.com/index.php/IJET*

***Research paper***

# Hollow Triangular Cross-Section Calculating Precast-Monolithic Beams Methods with Account for Concrete Nonlinear Properties

**Taliat Azizov[1]*, Dmitriy Kochkarev[2], Tatyana Galinska[3], Nadzieja Jurkowska[4]**

[1]*Pavlo Tychyna Uman State Pedagogical University, Ukraine*
[2]*National University of Water and Environmental Engineering, Ukraine*
[3]*Poltava National Technical Yuri Kondratyuk University, Ukraine*
[4]*Tadeusz Kosciuszko Cracow University of Technology, Poland*
**Corresponding author E-mail: dim7@ukr.net*

**Abstract**

The article examines precast-monolithic reinforced concrete beams with a cross section in the form of a hollow triangle. The advantages of such beams are presented and say that their stiffness in torsion is ten times bigger than the similar rigidity of a T-beam with the same stiffness and bending resistance. The article introduces the method of manufacturing such beams without the use of form work which was developed by the author of the article. Earlier the authors investigated the stiffness of such beams in torsion and it is mentioned in the article. However, stiffness and bending resistance are not investigated. Resistance and stiffness of precast-monolithic beams under bending differs from the resistance and stiffness of the monolithic ones. Consequently, taking into account the nonlinear properties of materials the calculation of such beams is different. The method for calculating beams under bending is introduced and it is based on the application of the flat section hypothesis. This method is used in conventional methods of calculation. The difference from the traditional calculation is the addition of equilibrium stress to the equations which are perceived by sections of monolithic concrete with physical and mechanical characteristics that differ from those of the main part of the structure. In calculation the cross-section of the beam is reduced to the equivalent T-section. The obliquity of the side faces is taken into account and the thickness of the edge of the equivalent T-beam is understood as the doubled thickness of the side edge divided by the sine of the angle of obliquity of the edges. In order to apply this calculation method, at first, it is necessary to check the sufficiency of the presence of a transverse reinforcement in the grid which is laid in the construction of the structure. With a sufficient diameter and rod spacing of transverse reinforcement which are calculated according to the authors' previously developed method, the structure can be calculated as monolithic with sections with different material characteristics according to the method introduced in the article. The calculations based on the above procedure showed a good match with the results of experimental studies of the authors.

***Keywords***: *Prefabricated monolithic beam, hollow triangle, hypothesis of plane sections, diagram, iteration.*

## 1. Introduction

It is known that taking into account the spatial work of reinforced concrete floors provides significant savings in materials and significantly improves the accuracy of determining the forces acting in the floor elements [1]. Analysis of various types of overlap shows that the spatial work of the latter, consisting of plates of type T or TT, is the smallest. This is due to the low torsional rigidity of such plates. In [2] it was shown that the overlap of T or TT plates can be replaced by overlaps of beams-slabs of triangular cross section. Such beams combine the functions of beams and slabs (Fig. 1).

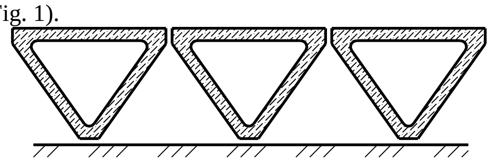

**Fig. 1:** Overlap hollow triangular section prefabricated plates cross section

The manufacture of T-shaped and I-beams is associated with the difficulties of making formwork. A beam with a cross-section shown in fig. 1 has all the advantages of T-beams, but at the same time it has a torsional rigidity ten times greater than the rigidity of a similar T-beam [2]. In order to simplify and reduce the cost of manufacturing such beams, it was proposed to manufacture them without the use of formwork in the form of a monolithic assembly. A diagram of the beam cross section in the monolithing position is shown in fig. 2

After curing concrete sections and monolithic sections 9 beam is ready for use. It turns over to the working position so that the working reinforcement is in the stretched zone. Such a beam combines the functions of the truss structure and plate, as the width of the compressed shelf can be freely taken 1.5 meters or more. The torsional stiffness of such a beam is much greater than that of a T-beam with the same strength and bending stiffness in the vertical direction. The last factor is a very, very significant advantage, since the greater the torsional rigidity, the more pronounced the effect of spatial work under the action of local loads.

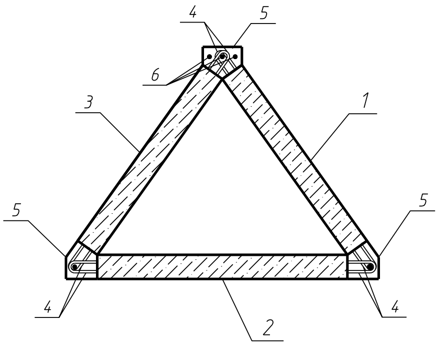


**Fig. 2:** Prefabricated monolithic reinforced concrete beam hollow triangular shape cross-section. 1, 2, 3 beam sides; 4- starter bars 5 - monolithic areas; 6 - working reinforcement

In [2], the torsional rigidity of such beams was investigated. It also shows the principle of calculating such beams during bending. However, the question of calculating such beams, taking into account the nonlinear properties of concrete, remains unexplored.

# 2. Hollow triangular cross-section precast-monolithic beams calculating methods during bending, taking into account materials nonlinear properties

## 2.1. Methods for calculating hollow triangular cross-section precast-monolithic beams during bending, considering the materials nonlinear properties

For the calculation taking into account materials nonlinear properties, the deformation method are used [3, 4, 5, 6, 7]. The calculated beam cross section is shown in Fig. 3.

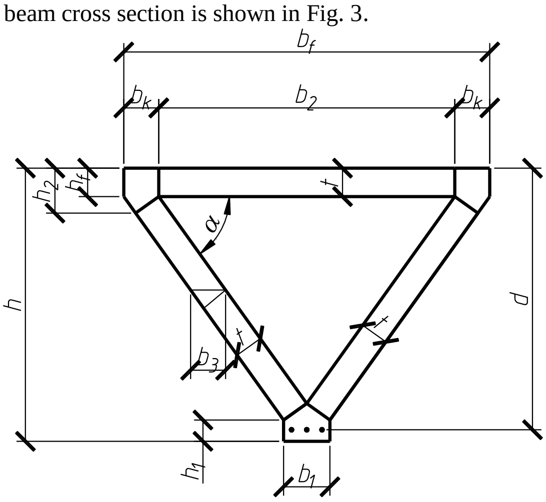


**Fig. 3:** Element in the form of a hollow triangle section diagram

Monolithic areas in the upper zone width $b_k$ and in the lower width $b_1$ have physical and mechanical characteristics that are different from the characteristics of the main beam sides. For the calculation of torsion, the section is considered in its original form. To calculate the bend in the form of a hollow triangle, it can be replace the T-section (Fig. 4). The width of the edge brand is equal to twice value (Fig. 4). $b_3$, being the horizontal projection of thickness t element sides (Fig. 3). It can be seen easily that $b_3=t/\sin\alpha$, where $\alpha$ – element lateral sides angle (Fig. 3).

Since the end parts of the shelf brand are made of concrete with different characteristics, it is possible to carry out calculations for the two-layer element similarly to the method [4]. The preliminary calculations of the authors carried out by this method displayed that, due to the small width of the monolithic sections $b_k$ the section can be considered as a solid with a shelf width $b_f=b_2+2b_k$ (Fig. 3).

In addition, as shown by calculations based on the methodology [1], at a certain step and diameter of the grid bars, the beam can be considered monolithic.

For calculation, the T-section should be divided into a number of horizontal layers with a thickness *a* (Fig. 4). Layers can be either the same thickness or different.

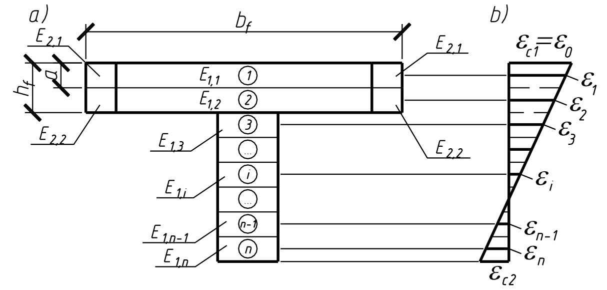


**Fig. 4:** Reduction of a hollow triangle to a T-section: a) cross section; b) epyura longitudinal deformations

The calculation is carried out according to an algorithm similar to [3, 4] with some changes related to the presence of various materials in the section. Let us dwell on these differences. For calculation at zero iteration, a certain deformation of a compressed extreme compressed fiber is set. $\varepsilon_{c1}$ first layer (Fig. 4). Deformation on the bottom side of the last layer with the number *n* (Fig. 4) is taken equal to zero $\varepsilon_{c2}=0$.

Further, the curvature in cross section is calculated by the formula:

$$1/r=\frac{\varepsilon_{c1}-\varepsilon_{c2}}{h}. \tag{1}$$

At the level of every *i*-layer, based on the linear distribution of deformations (Fig. 4, b), the deformation of this layer is determined $\varepsilon_i$. According to acquainted diagrams *"σ-ε"* определяются текущие значения модуля деформаций в этом слое для основного бетона determined by the current values of the modulus deformations in this layer for the main concrete $E_{1,i}$ and concrete grouting $E_{2,i}$. In each layer, the efforts are determined. $N_i$ by formula:

$$N_i=\varepsilon_i\left[E_{1,i}A_{1,i}+E_{2,i}A_{2,i}+E_{s,i}A_{s,i}\right]. \tag{2}$$

where $A_{1,i}$ and $A_{2,i}$ – layers cross-sectional area of the layers, respectively, for the main concrete and concrete grouting; $E_{s,i}$, $A_{s,i}$ – respectively, the modulus of elasticity and the cross section of reinforcement i-layer.

Signs $N_i$ are taken in accordance with the signs of the deformation plot: compression is a positive sign, tension is negative.

Square $A_{1,i}$ and $A_{2,i}$ are determined from expressions (Fig. 3, 4):

$$A_{1,i}=2\cdot a\,\frac{t}{\sin\alpha};\ A_{2,i}=2\cdot b_k\cdot a. \tag{3}$$

If the width of the monolithic section in the lower zone (Fig. 3) larger $2b_3$, then the areas of these layers are adjusted accordingly. If the layers along the section height have different thickness, then in expression (3) instead of *a* it should be taken $a_i$.

Expression (2) differs from the similar expressions [3, 4] by the presence of the second terms $E_{2,i}$ and $A_{2i}$, which take into account the presence of the second component for monolithic concrete in cross section. Moreover, if for the i- layer the inequality $i\cdot a>h_f$, if the layer is below the shelf of the element, then in expression (2) is taken $E_{2,i}=0$ и $A_{2i}=0$.

Next, the total force in the cross section is calculated. If it is greater than zero, then at the next iteration a tensile strain is added. $\varepsilon_{c2}$ and the calculation is repeated. Thus, the further algorithm does not differ from the acquainted algorithm [4], and therefore in the article is not given further.

The advantage of this approach to the calculation is the fact that the calculation takes into account the various characteristics of precast materials and monolithic materials, and can also be taken into account reinforcing bars not only of the main working reinforcement, but also the longitudinal bars of the mesh, which are placed in the element lateral sides in a horizontal position.

To clarify the calculations can be at the level (top to bottom)$h_2 \leq i \cdot a \geq h_f$ to take into account that in this layer, the areas of the main concrete and the concrete hardening vary, and they can be easily calculated from geometrical considerations ( Fig. 3).

It should be noted that in order for the precast-monolithic beam to be counted as monolithic (without taking into account the shelf shift relative to the ribs), it is necessary to carry out calculations according to the method [1] and take a certain diameter and step of the transverse mesh reinforcement in the manufacture of the beam. With a smaller diameter or reinforcement spacing, consideration should be given to the possibility of shifting the flange relative to the rib and reducing the total force in the compressed zone according to [1].

The calculations by the above method showed proper correlation with the authors' experimental studies.

### 2.2. Hollow triangular cross-section precast-monolithic beams calculating method during bending using imputed concrete resistances

The calculation of hollow triangular section beams can be made using the method of imputed reinforced concrete resistance, which is described in detail in [8, 9, 10]. For the calculation of reinforced concrete elements using this method, non-linear materials deformation diagrams, the hypothesis of deformations linearity, as well as the corresponding criteria for the formation of cracks and fracture is used. Calculation formulas for the convenience of calculations are reduced to the formulas of material classical resistance. The main parameters of the stress-strain state are summarized in tabular form. The strength of T-sections of reinforced concrete elements is determined based on the following condition

$$\frac{M_{Ed}}{W_c} \leq f_{zM}, \tag{4}$$

where $f_{zM} = f($concrete type, $\rho_f$, $f_{yd})$ – the calculated resistance of reinforced concrete is determined by the relevant tables [8]; $W_c$ – elastic moment of resistance to the cross section of concrete. Table 1 shows the value of the calculated resistance reinforced concrete, calculated for reinforced concrete elements of rectangular cross-section with a single reinforcement, while the formula proposed in the Eurocode 2 was used as concrete deformation diagram [3].

To determine the strength of the cross section using formula (4), it is necessary to know in advance the position of the neutral line in the cross section. In the case, each section is calculated twice: a T-profile element with a moment of resistance $W_t$ and an element of rectangular cross section $b_f \times d$ with moment of resistance $b_f \times d^2/6$.

Of the two values obtained, when determining the area of reinforcement, they take a larger value, and when calculating the bearing capacity, it is less.

The deflections of T-reinforced concrete elements by the method of imputed resistance reinforced concrete are calculated using the curvature of the sections. In this case, it is used to determine the deflections Mohr integral or the Simpson formula. In some cases, for the preliminary determination of the deflections, it is possible to use an approximate formula. In it, the deflection is determined by the same curvature value found in the cross section with the greatest moment.

**Table 1:** Reinforced concrete estimated resistance $f_{zM}$ with single reinforcement

| Concrete class | Proportion of reinforcement, $\rho_f$ | | | | | | | |
|---|---|---|---|---|---|---|---|---|
| | **0.05** | **0.50** | **1.00** | **1.25** | **1.50** | **1.75** | **2.00** | **3.00** |
| | ***$f_{yd}$=375 МПа (A400C)*** | | | | | | | |
| **C8/10** | 1.10 | 9.44 | 14.68 | 15.12 | 15.43 | 15.67 | 15.86 | 16.32 |
| **C12/15** | 1.11 | 9.97 | 17.38 | 20.09 | 20.85 | 21.27 | 21.60 | 22.45 |
| **C16/20** | 1.11 | 10.30 | 18.70 | 22.19 | 25.20 | 27.38 | 27.90 | 29.29 |
| **C20/25** | 1.11 | 10.49 | 19.48 | 23.40 | 26.95 | 30.11 | 32.88 | 35.65 |
| **C25/30** | 1.11 | 10.60 | 19.91 | 24.08 | 27.93 | 31.46 | 34.66 | 40.69 |
| **C30/35** | 1.12 | 10.68 | 20.24 | 24.59 | 28.66 | 32.45 | 35.96 | 45.45 |
| **C32/40** | 1.12 | 10.75 | 20.49 | 24.98 | 29.23 | 33.22 | 36.96 | 49.26 |
| **C35/45** | 1.12 | 10.81 | 20.72 | 25.35 | 29.76 | 33.94 | 37.90 | 51.52 |
| **C40/50** | 1.12 | 10.84 | 20.88 | 25.60 | 30.11 | 34.42 | 38.53 | 52.94 |
| **C45/55** | 1.12 | 10.87 | 21.01 | 25.80 | 30.40 | 34.82 | 39.05 | 54.10 |
| **C50/60** | 1.12 | 10.90 | 21.14 | 26.00 | 30.69 | 35.21 | 39.56 | 55.26 |
| | ***$f_{yd}$=450 МПа (A500C)*** | | | | | | | |
| **C8/10** | 1.32 | 10.90 | 14.57 | 15.02 | 15.35 | 15.60 | 15.79 | 16.27 |
| **C12/15** | 1.33 | 11.66 | 19.40 | 20.15 | 20.70 | 21.13 | 21.48 | 22.35 |
| **C16/20** | 1.33 | 12.13 | 21.53 | 25.17 | 26.50 | 27.16 | 27.71 | 29.13 |
| **C20/25** | 1.33 | 12.41 | 22.65 | 26.95 | 30.69 | 32.67 | 33.42 | 35.43 |
| **C25/30** | 1.34 | 12.57 | 23.28 | 27.93 | 32.12 | 35.82 | 37.89 | 40.40 |
| **C30/35** | 1.34 | 12.69 | 23.74 | 28.66 | 33.18 | 37.28 | 40.93 | 45.10 |
| **C32/40** | 1.34 | 12.78 | 24.11 | 29.23 | 33.99 | 38.39 | 42.40 | 49.53 |
| **C35/45** | 1.34 | 12.86 | 24.44 | 29.76 | 34.75 | 39.42 | 43.78 | 54.52 |
| **C40/50** | 1.34 | 12.92 | 24.67 | 30.11 | 35.26 | 40.11 | 44.68 | 58.52 |
| **C45/55** | 1.34 | 12.96 | 24.86 | 30.40 | 35.68 | 40.69 | 45.43 | 61.40 |
| **C50/60** | 1.34 | 13.01 | 25.04 | 30.69 | 36.10 | 41.25 | 46.17 | 63.37 |

The elastic moment of concrete resistance is determined depending on the position of the neutral line in the section:

- When the position of the neutral line in the edge

$$W_c = \frac{b_f d^2}{6}; \tag{5}$$

- When neutral line position in the shelf

$$W_{ct} = \frac{b_f d^2}{6} - \frac{(b_f - b)(d - h_f)^2}{6}. \tag{6}$$

In general, the curvature can be found by the formula

$$1/r = \frac{\sum \varepsilon}{d}, \tag{7}$$

where $\sum \varepsilon$ – the sum of deformations in compressed concrete and tensile reinforcement.

The total deformations of the concrete depend on the following parameters.

$$\sum\varepsilon = f(\rho_f, \sigma_{zM}, C, A), \quad (8)$$

where $\sigma_{zM} = \dfrac{M}{W_c}$ – conditional stresses in the cross section of a reinforced concrete element. The sum of compressed concrete deformations and tensile reinforcement can be found using appropriate tables. A fragment of such a table is shown below (Table 2).

**Table 2:** Stress-strain state parameters

| Concrete class | Load level | Proportion of reinforcement, $\rho_f$ | | | | | |
|---|---|---|---|---|---|---|---|
| | | 0.5 | | | 1 | | |
| | | $\sigma_{zM}$, MPa | $\sum\varepsilon$ $\times10^4$ | $\sigma_s$, MPa | $\sigma_{zM}$, MPa | $\sum\varepsilon$ $\times10^4$ | $\sigma_s$, MPa |
| C20/25 | $M_{W1}$ | 3.4 | 2.9 | 31.9 | 4.1 | 3.0 | 31.8 |
| | $M_{W2}$ | 3.4 | 4.4 | 101.6 | 4.1 | 4.4 | 63.0 |
| | 0.4 | 6.8 | 12.5 | 243.1 | 8.5 | 10.7 | 155.4 |
| | 0.6 | 9.1 | 18.1 | 329.1 | 12.8 | 16.9 | 239.4 |
| | 0.8 | 11.0 | 26.4 | 398.9 | 20.8 | 31.5 | 400.0 |
| | 1.0 | 11.3 | 126.5 | 400.0 | 21.3 | 72.4 | 400.0 |
| C25/30 | $M_{W1}$ | 4.0 | 3.0 | 33.8 | 4.7 | 3.2 | 33.7 |
| | $M_{W2}$ | 4.0 | 4.7 | 118.6 | 4.7 | 4.7 | 72.2 |
| | 0.4 | 6.9 | 11.4 | 240.9 | 8.7 | 10.1 | 155.9 |
| | 0.6 | 9.1 | 16.8 | 329.0 | 13.0 | 16.2 | 241.4 |
| | 0.8 | 11.1 | 26.1 | 398.8 | 21.3 | 32.7 | 400.0 |
| | 1.0 | 11.4 | 137.9 | 400.0 | 21.7 | 77.7 | 400.0 |

### 2.3. Hollow triangular cross-section precast-monolithic beams deflection calculating method during bending using linearization dependencies

The above proposed method of design resistances of reinforcement concrete makes it possible to significantly simplify the determination of reinforced concrete elements deflections. To do this, you must perform a linearization dependency.

$$\sigma_{zM} = a_i + b_i \sum\varepsilon, \quad (9)$$

where $a_i$, $b_i$ – linearized dependencies parameters.

The linearization of the parameters of the stress-strain state should be carried out from the moment of the formation of cracks until the onset of the yield stress in the stretched armature. This will make it possible to find deflections with accuracy sufficient for engineering practice at operational loads. The linearization coefficients obtained in this way for the main classes of concrete, and reinforcement percentages of 0.5–3%, are presented in Table 3. It is worth noting about the high degree of approximation of the obtained straight lines within the specified limits, constructed using formula (9). So the correlation coefficients of straight lines are within 0.956-0.98.

Using formula (9) it is easy to obtain a linearized curvature formula

$$1/r_x = \frac{M_x}{b_i W_{ct} d} + \frac{a}{b_i d}. \quad (10)$$

To find the deflections, it is necessary to write down the Mohr integral or Simpson's formula for the corresponding computational scheme, and obtain the necessary formula. For some of the most common calculation schemes, the formulas for finding the maximum deflections using linearization parameters are presented in Table 4.

**Table 3:** To the calculation of deflections of bending reinforced concrete elements using linearization dependencies

| **Concrete class** | ***a*, MPa** | **Proportion of reinforcement, $\rho_f$** | | | |
|---|---|---|---|---|---|
| | | **0.5** | **1** | **2** | **3** |
| | | ***$b_i$*, $10^{-4}$ MPa** | | | |
| **C8/10** | 1.845 | 0.262 | 0.410 | 0.614 | 0.764 |
| **C12/15** | 2.116 | 0.301 | 0.484 | 0.741 | 0.929 |
| **C16/20** | 2.146 | 0.343 | 0.544 | 0.851 | 1.075 |
| **C20/25** | 2.256 | 0.355 | 0.598 | 0.929 | 1.175 |
| **C25/30** | 2.455 | 0.368 | 0.613 | 0.992 | 1.277 |
| **C30/35** | 2.701 | 0.374 | 0.644 | 1.024 | 1.315 |
| **C32/40** | 2.769 | 0.396 | 0.663 | 1.038 | 1.376 |
| **C35/45** | 2.803 | 0.398 | 0.684 | 1.102 | 1.404 |
| **C40/50** | 2.843 | 0.419 | 0.706 | 1.148 | 1.475 |
| **C45/55** | 2.849 | 0.437 | 0.723 | 1.183 | 1.526 |
| **C50/60** | 3.188 | 0.452 | 0.725 | 1.201 | 1.563 |

**Table 4:** Deflection Formulas

| **№** | **Beam scheme** | **Formula for determining deflection** |
|---|---|---|
| 1 | 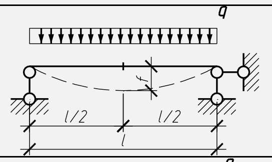 | $f = \frac{5}{384}\frac{ql^4}{b_i W_c d} - \frac{l^2}{8}\frac{a}{b_i d}.$ |
| 2 | 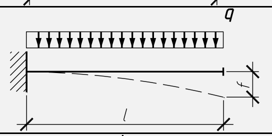 | $f = \frac{1}{8}\frac{ql^4}{b_i W_c d} - \frac{l^2}{2}\frac{a}{b_i d}.$ |
| 3 | 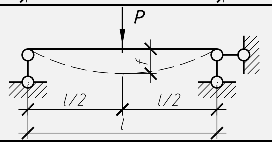 | $f = \frac{1}{48}\frac{Pl^3}{b_i W_c d} - \frac{l^2}{8}\frac{a}{b_i d}.$ |

## 3. Interaction forces between the shelf determination and inclined sides in beams of hollow triangular cross section

The peculiarity of composite-monolithic beams calculations hollow triangular cross-section lies in the fact that they cannot always be calculated as elements of a continuous section due to the presence of a monolithic seam. If the rigidity of the monolithic seam is high enough, then it can be calculated as a monolithic structure by the method described above.

The presence of a monolithic seam between the flange and the edge (two inclined elements that constitute the edge of the beam) turns such a beam into a composite with flexible shear links. Its calculation can be carried out in the first approximation by the composite rods A.R. Rzhanitsyna theory [11]. However, when calculating to the nonlinear properties of a monolithic concrete, the calculation according to the theory of composite rods [11] is difficult, since in the theory of composite rods, the plastic properties of shear bonds are taken into account only when subjecting the Prandtl diagram.

This disadvantage can be avoided by counting the beam in the form of a rod system shown in Fig. 5. In this figure it is indicated: 1 - upper shelf; 3 - edge (side flanges of the beam); 2 - links that imitate the work of a monolithic seam between the shelf and the edge. The number and pitch rods 2, imitating the work of a monolithic seam can be selected by preliminary calculation.

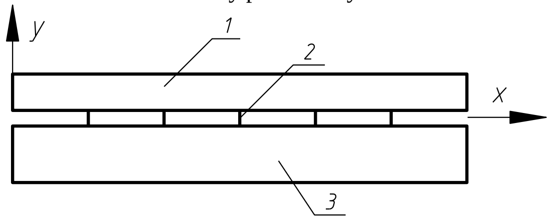


**Fig. 5:** Composite monolithic two-layer beam scheme

It is known [10] that in two-layer composite beams, the elasticity of cross-links can be neglected and considered as absolutely rigid. Thus, if we assume that in the vertical direction rods 1 and 3 have the same displacements, then the accuracy of the calculation will not suffer. The factor is taken into account when developing the method for calculating the beams under consideration. If communications 2 on fig. 5 in the transverse direction are not deformed, then the rods 1 and 3 will bend along the same curve. The main system can be improved by dissecting cross-links and considering the consistency of horizontal displacements of rods 1 and 3. That is, displacements along the X axis of the lower side of the upper rod are equal to the displacements of the upper side of the lower rod, corrected for the shear of cross-links.

Let it *2n* connections between rods. Split the beam into sections $a_t = l/(2n)$ . And the arrangement of communications will be symmetric as shown in fig. 6. If only the condition of compatibility horizontal displacements is taken into account, then after the thoughtful dissection of the connections, the main system and unknown forces will have the form shown in (fig. 6). Let the beam acts uniformly distributed load. *q*. Then by virtue of symmetry instead of *2n* it will be *n* indeterminate (Fig. 6).

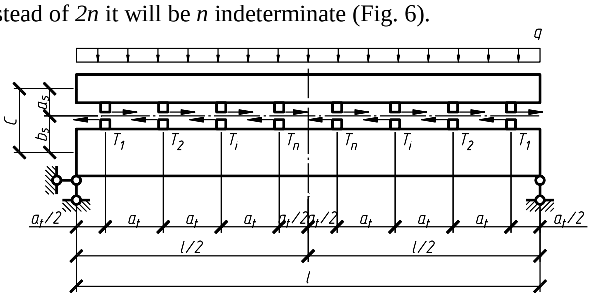


**Fig. 6:** Unknown forces after cutting a beam into two rods

Now it is proceed directly to the derivation of equations system for determining unknown forces. $T_i$. To determine the movement along the axis *x* first are the angles of rods rotation.

1. Beam angles at i-point

$$\varphi_i = \frac{ql^3}{24EI_{tot}}\alpha_i, \tag{11}$$

where the index i denotes the location number of the connection (i=1, 2, 3, …n);

$$\alpha_i = 1 - 6\left(\frac{a_i}{l}\right)^2 + 4\left(\frac{a_i}{l}\right)^3, \tag{12}$$

$a_i$ – distance from the origin (left support of the beam) to the i-point:

$$\alpha_i = \frac{a_t}{l} + (i-1)a_t; \tag{13}$$

$EI_{tot}$ – the upper and lower rods flexural stiffness sum.

Move the lower face of the upper rod

$$\Delta_i^V = -\varphi_i a_s; \tag{14}$$

Перемещения верхней грани нижнего стержня:

Move the upper side of the lower rod

$$\Delta_i^n = \varphi_i b_s, \tag{15}$$

where $a_s, b_s$ – the distance from the seam between the beams, respectively, to the upper and lower rods (see Fig. 6). The angle of rotation according to (11) and (12) is determined by the familiar formula for the resistance of materials [12].

2. Angles of rotation from the action of moments created by unknown forces $T_i$

$$\varphi_i = \frac{c}{EI_{tot}}\Big(\alpha_{i1}^M T_1 + \alpha_{i2}^M T_2 + ...\alpha_{in}^M T_n - $$
$$-\alpha_{i1}^r T_1 - \alpha_{i2}^r T_2 - ... - \alpha_{in}^r T_n\Big) \tag{16}$$

where $\alpha_{ij}^M$ – the coefficient to determine the angle of rotation of the beam at point i from the force applied at point j and to the left of the mid-span of the beam;.

Coefficients $\alpha_{ij}^M$ are determined by the formulas:

$$\alpha_{ij}^M = \frac{a_i^2}{2l} + \frac{a_j^2}{2l} + \frac{l}{3} - a_j, \; i \le j; \tag{17}$$

$$\alpha_{ij}^M = \frac{a_i^2}{2l} + \frac{a_j^2}{2l} + \frac{l}{3} - a_i, \; i \le j. \tag{18}$$

Difference in definition $\alpha_{ij}^M$ from $i \le j$ consists in the fact that under the action of the concentrated moment in the beam according to the scheme in fig. 7 is determined by the formulas [12]:

- Location on
 $0 \le x \le a$

$$y^I = \varphi = \frac{M}{EI_{tot}}\left(\frac{x^2}{2l} + \frac{a^2}{2l} + \frac{l}{3} - a\right); \tag{19}$$

- Location on $a \le x \le l$

$$y^I = \varphi = \frac{M}{EI_{tot}}\left(\frac{x^2}{2l} + \frac{a^2}{2l} + \frac{l}{3} - x\right). \tag{20}$$

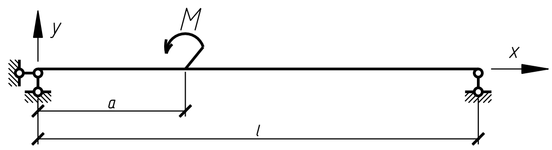


**Fig. 7:** The design scheme for determining the angle of rotation in the beam with co-focused moment

Expressions (19) - (20) are derived by the formulas of the resistance of materials [11].

The coefficients from the action of forces to the right of the middle of the beam are determined by the formula

$$\alpha_{ij}^r = \frac{a_i^2}{2l} + \frac{a_{j,r}^2}{2l} + \frac{l}{3} - a_{i,r}, \tag{21}$$

where $\alpha_{j,r}^r$ – the distance from the origin to the force to the right of the middle of the beam (see Fig. 8).

Movement the lower side of the upper rod

$$\Delta_i^V = \varphi_i a_s. \tag{22}$$

Movement the upper side of the upper rod

$$\Delta_i^n = -\varphi_i b_s, \tag{23}$$

here, the signs are taken as opposite signs according to (14) and (15), since from the action of moments $M_i = T_i C$ the points of the lower side of the upper rod move to the right, and the points of the upper side of the lower rod move to the left.

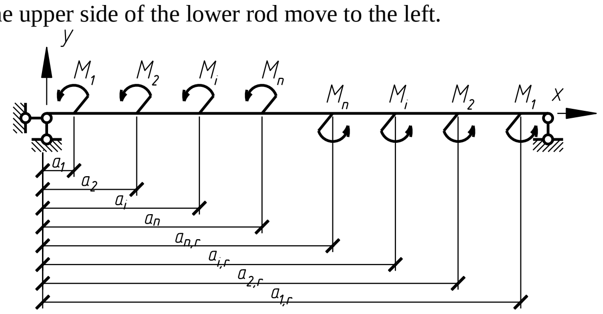


**Fig. 7:** Scheme for determining distances to unknown moments

3. Displacement from compression-tension of rods by forces $T_i$ :

$$\Delta_i^V = \frac{1}{EA_V}\left(\alpha_{i1}^T T_1 + \alpha_{i2}^T T_2 + ...\alpha_{in}^T T_n\right); \tag{24}$$

$$\Delta_i^n = -\frac{1}{EA_n}\left(\alpha_{i1}^T T_1 + \alpha_{i2}^T T_2 + ...\alpha_{in}^T T_n\right); \tag{25}$$

where $EA_V$ и $EA_n$ – respectively, the axial stiffness of the upper and lower rods; $\alpha_{ij}^T$ determined by the formulas (Fig. 8):

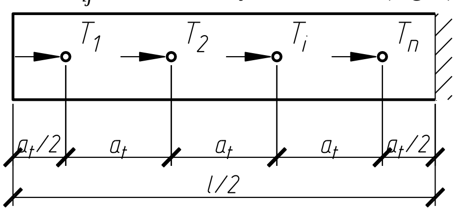


**Fig. 8:** Scheme for determining displacements from compression of rods by unknown forces $T_i$

$$\alpha_{ij}^T = (n-i)a_t + \frac{a_t}{2},\ i \le j; \tag{26}$$

$$\alpha_{ij}^T = (n-j)a_t + \frac{a_t}{2},\ i > j. \tag{27}$$

4. Displacement from shear relationships. For simplicity, it is assume that each bond is deformed independently of its neighbors (like the calculation of beams on an elastic base, when the elastic base is represented by a system of unrelated springs)

$$\Delta_i^V = \frac{S}{Gtd}T_i;\ \Delta_i^n = -\frac{S}{Gtd}T_i; \tag{28}$$

where *G* – bond concrete shear modulus; *S, t, d* – respectively, half the height, thickness and width of the bond (section of the monolithic seam of the beam). In our case $d=a_t$.
The condition of compatibility deformations will be written as $\Delta_i^V = \Delta_i^n$, so it should be equated the sum of all expressions $\Delta_i^V$ by formulas (14), (22), (24) and (28) the sums of expressions $\Delta_i^n$ by formulas (15), (23), (25) и (28).
As a result, it will be obtained linear equations system:

$$\begin{cases} a_{11}T_1 + a_{12}T_2 + ... + a_{1n}T_n = b_1 \\ a_{21}T_1 + a_{22}T_2 + ... + a_{2n}T_n = b_2 \\ ...\ ...\ ...\ ...\ ...\ ...\ ...\ ...\ ...\ ... \\ a_{n1}T_1 + a_{n2}T_2 + ... + a_{nn}T_n = b_n \end{cases}; \tag{29}$$

where

$$\alpha_{ij} = \left(a_{ij}^M - a_{ij}^r\right)\frac{C^2}{EI_{tot}} + a_{ij}^T\left(\frac{1}{EA_V} + \frac{1}{EA_n}\right) + \frac{2S}{Gtd}; \tag{30}$$

$$b_i = \alpha_i \frac{ql^3C}{24EI_{tot}}. \tag{31}$$

As a result of solving equations system (29), all unknown forces will be found $T_i$ , after it the forces and displacements of the beam are determined by the known formulas of the materials resistance against the action of an external load and moments $M_i = T_iC$ .
In the absence of compliance shear ties, the last term of expression (30) turns into zero and the beam is considered as monolithic with a total section height equal to the sum of the heights of the upper and lower rods.
The advantage of the proposed calculation method is the possibility of taking into account the nonlinear properties of shear bonds (monolithic seam), since the rigidity of each bond may be different. In this case, instead of the last term of expression (30), which is a constant for all points, there will be an expression $\frac{2S}{G_it_id_i}$, so at each point, the shear stiffness (shear modulus, thickness, and width of the bond) is different. This stiffness is determined by iterative calculation depending on the workload of the *i* shear connection by known methods.
The number of sections where the length of the beam should be divided is selected by preliminary calculation and usually 15–20 sections are sufficient for quite acceptable calculation accuracy.
Thus, a method for determining the forces in the monolithic seam between the shelf and the ribs of the beam under consideration has been developed, which enables to take into account the nonlinear properties of the concrete for monolithing. The technique is based on the prerequisites of composite rods theory, but differs in the possibility of using any laws of deformation in a monolith seam, which is practically impossible in the composite rods theory.
If the rigidity of the connections is sufficiently large, then the beam can be considered as monolithic and calculated using the method described above. To determine the stiffness of the bond, where a beam can be considered monolithic, several calculations should be carried out with a gradual increase in the stiffness of the bonds. If at the last and previous stage of increasing the rigidity of the bonds, the efforts differ little from each other, the rigidity of the bonds can be considered conditionally infinite and the beam can be considered as monolithic.

## 4. Hollow triangular cross-section floors consisting of beams calculations, taking into account the spatial work

Let an overlap consisting of *n* hollow triangular cross section beams be given. In general, the overlap with beams in one direction looks as shown in Figure 9.
It will be cut the overlap into separate beams of a hollow triangular section with planes parallel to the longitudinal axes (Fig. 9) and used the method of spatial calculation [2].

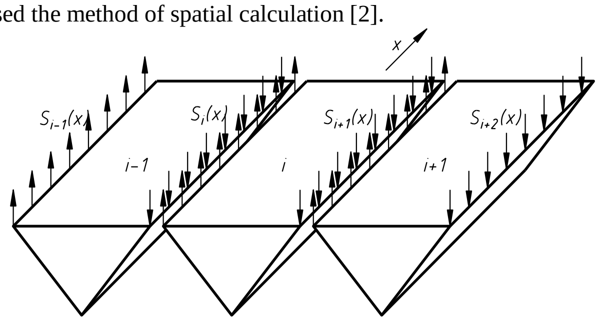


**Fig. 9:** Scheme for the calculation of the overlap with the spatial work

In the above-mentioned method [2], in the general case, four component forces of interaction act on the overlapping cut-off lines into individual beams. To calculate the system we are considering, it is quite sufficient to use a method that takes into account only the presence of vertical efforts of the interaction of the beams with each other. For this purpose, from the general system of differential equations [2], it is necessary to leave only the terms containing the vertical forces of interaction *S(x)*. The system of differential equations in this case is:

$$\begin{aligned}
&-\frac{1}{EI_i}\cdot MS_{i-1}+\left(\frac{1}{EI_i}+\frac{1}{EI_{i+1}}\right)\cdot MS_i+\frac{1}{EI_{i+1}}\cdot MS_{i+1}+\\
&+\frac{L_i\cdot R_i}{GI_i}\cdot MS''_{i-1}+\left(\frac{R_i^2}{GI_i}+\frac{L_{i+1}^2}{GI_{i+1}}\right)\times\\
&\times MS_i''+\frac{L_{i+1}\cdot R_{i+1}}{GI_{i+1}}\cdot MS_{i+1}''+\left(\frac{R_i^3}{3D_i}+\frac{L_{i+1}^3}{3D_{i+1}}\right)\cdot MS_i^{iv}=\\
&=\frac{1}{EI_{i+1}}\cdot MQ_{i+1}-\frac{1}{EI_i}\cdot MQ_i,
\end{aligned}\tag{32}$$

where the following notation is used: $L_i$, $R_i$ – distances from the center of gravity the *i*-beam to the left and right sections; $EI_i$, $GI_i$ – Flexural rigidity of the beam, respectively, in vertical and horizontal directions; $EA_i$ – axial stiffness of the beam; $D_i$ – T beam cylindrical rigidity of the flange ;bi– vertical distance from the center of gravity of the beam section to the axis of the flange; $MS_i=MS_i(x)$ – bending moment function from unknown vertical forces $S_i(x)$, associated with the latest differential dependence $MS_i''(x)=S_i(x)$; $MQ_i=MQ_i(x)$ – function of bending moments from external load $q_i$.

In our case, the bending stiffness of the shelf can be taken equal to infinity, since the triangular cross section is fairly rigid and the curvature in the transverse direction can be neglected. With that said, equation (32) can be written as:

$$\begin{aligned}
&-\frac{1}{EI_i}\cdot MS_{i-1}+\left(\frac{1}{EI_i}+\frac{1}{EI_{i+1}}\right)\cdot MS_i+\frac{1}{EI_{i+1}}\cdot MS_{i+1}+\\
&+\frac{L_i\cdot R_i}{GI_i}\cdot MS''_{i-1}+\left(\frac{R_i^2}{GI_i}+\frac{L_{i+1}^2}{GI_{i+1}}\right)\times\\
&\times MS_i''+\frac{L_{i+1}\cdot R_{i+1}}{GI_{i+1}}\cdot MS_{i+1}''=\frac{1}{EI_{i+1}}\cdot MQ_{i+1}-\frac{1}{EI_i}\cdot MQ_i,
\end{aligned}\tag{33}$$

System (33) can be conveniently solved using the Fourier series expansion in sinuses:

$$MS_i(x)=\sum_{n=1}^{\infty}MS_{n,i}\cdot\sin\alpha x\,;\;MQ_i(x)=\sum_{n=1}^{\infty}MQ_{n,i}\cdot\sin\alpha x\,,\tag{34}$$

where - for multiplicity indicated $\alpha=\frac{\pi\cdot n}{l}$; $x$ – coordinate along overlap span beam; $l$ – span beam;

Substituting (34) into (33), making a differentiation and reducing by *Sin(αx)*, instead of a system of differential equations, will obtain a system of linear finite equations, which in this case have the form:

$$\begin{aligned}
&\left(-\frac{1}{EI}+\frac{a^2\cdot\alpha^2}{GI}\right)\cdot MS_{n,i-1}+\left(\frac{2}{EI}+\frac{2a^2\cdot\alpha^2}{GI}\right)\cdot MS_{n,i}+\\
&+\left(-\frac{1}{EI}+\frac{a^2\cdot\alpha^2}{GI}\right)\cdot MS_{n,i+1}=\frac{1}{EI}\left(-MQ_{n,i}+MQ_{n,i+1}\right).
\end{aligned}\tag{35}$$

Equations (35) should be written for each seam of the overlap. After determining the efforts of beams interaction with each other, each i- beam with its own external load and interaction efforts on the left $S_i$ and on the right $S_{i+1}$ (fig. 10).

In fig. 10 at the ends of the beam, the connections preventing the beam from turning around the longitudinal axis are shown. This is due to the fact that the ends of adjacent beams are interconnected, which prevents their rotation around the longitudinal axis. Efforts $S_i(x)$ have zero values on the supports (see fig. 10), since functions change them are functions of the sinuses. This is justified for the following reason. The supports of the beams at their ends are rigid and in this place the beams cannot move relative to each other. Therefore, the efforts of shifting one beam relative to another will be absent.

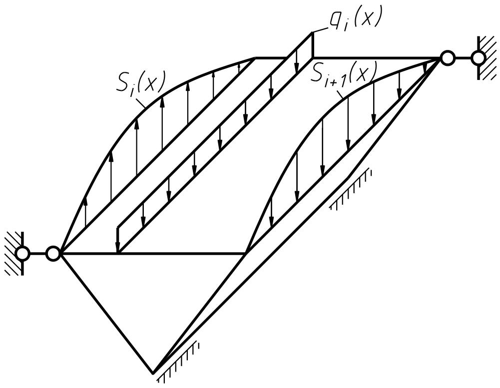


**Fig. 10:** Forces diagram acting on the studied i- beam

Thus, the first stage of the overlap calculation, consisting of hollow triangular cross-section beams, is the calculation of its spatial work according to the above method in order to determine the efforts of individual beams interaction with each other. After that, one should proceed to the calculation of the stiffness and strength of each beams, which are exerted by external loads and the forces of interaction applied to their edges (see Fig. 10). As calculation result, the presence of cracks is checked, the stiffness characteristics of the flange and the side edges of the beam are changed, as well as its rigidity as a whole, and the calculation of the joint operation of all the beams is repeated using the above method, but with the modified stiffness characteristics.

## 5. Hollow triangular cross-section precast-monolithic beams calculation examples while bending

Consider precast-monolithic beams with triangular cross-section calculation examples at bending.

Example1. Determine the strength of the section on the bend of the precast-monolithic beam shown in Fig.11. Class of concrete precast and monolithic parts C20/25. Reinforcement in constructive walls. The beam is calculated without taking into account the shift of the shelf relative to the ribs.

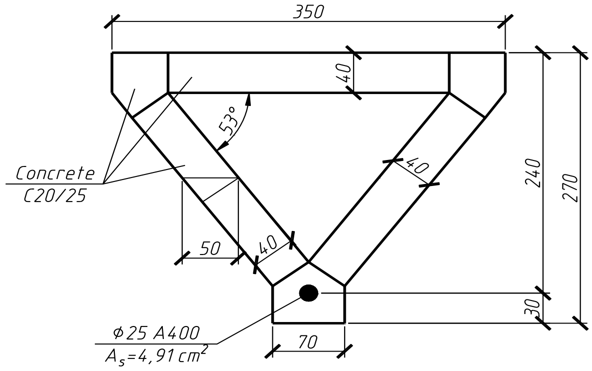


**Fig. 11:** Precast monolithic beam cross section

Solution.
Replace the hollow triangular cross section with the one shown below (fig.12).
Determine the moment of resistance for a rectangular section $b_f \times d$

$$W_c = \frac{b_f d^2}{6} = \frac{35 \times 24^2}{6} = 3360 cm^3.$$

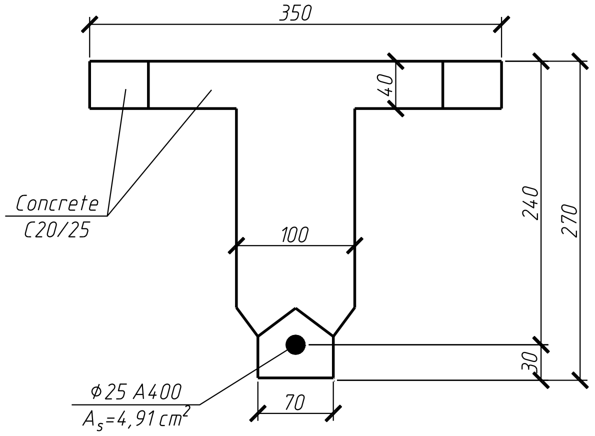


**Fig. 12:** Given precast monolithic beam cross section

Next, determine the percentage of reinforcement $\rho_f = \frac{A_s}{b_f d} = \frac{4.91}{35 \times 24} 100\% = 0,585\%.$

Using interpolation according to table 1, we find the calculated resistance of reinforced concrete $f_{zM} = 11.70\, MPa$ .

Find limiting bending moment value $M_{Ed} = f_{zM} W_c = 11.70 \times 3360 \times 10^{-3} = 39.31\, kN \cdot m.$

Find the resistance moment for the T-section

$$W_t = \frac{b_f d^2}{6} - \frac{(b_f - b_1)(d - h_f)^2}{6} = 169333\, cm^3.$$

Reinforcement percentage for T-section is $\rho_{f,t} = \frac{A_s}{b_1 d + (b_f - b_1) h_f} = 1.444\%.$

Find reinforced concrete calculated resistance according to table 1 $f_{zM,t} = 25.31\, MPa$ .

Bending moment limit value, when neutral line position in the edge

$$M_{Ed,t} = f_{zM,t} W_t = 25.31 \times 169333 \times 10^{-3} = 42.87\, kN \cdot m.$$

Out of two values $M_{Ed}$ и $M_{Ed,t}$ take less that is, the strength of a normal section is equal to $M$=39.31 kN·m.
As a result of the calculation of the beam by an iterative method, we obtained load bearing value $M$=39.66 kN·m, the difference is 0.88 %.
Example 2. Determine beam deflections (see Example 1) on two supports loaded with a uniformly distributed load (Scheme No. 1, Table 4) of a hollow triangular section shown in Fig. 5 with the following loads 0.9q=7.86 kN/m, 0.8q=6.99 kN/m, 0.7q=6.12 kN/m, 0.6q=5.24 kN/m. Beam has a span $l=6\ m$.
Solution.
Using table 3 determine the coefficients of linearization by interpolation, depending on the class of concrete C20/25 and reinforcement percentage $\rho_{f,t} = 1.444\%$ – $a=2.256$ *MPa;* $b_i=0{,}745 \times 10^4$ *MPa*.
Deflections calculation will be performed according to the formula of the linearization method (1, tab.4):

$$f_1 = \frac{5}{384} \frac{0.9ql^4}{b_i W_c d} + \frac{l^2}{8} \frac{a}{b_i d} = 3{,}813 cm;$$

$$f_2 = \frac{5}{384} \frac{0.8ql^4}{b_i W_c d} + \frac{l^2}{8} \frac{a}{b_i d} = 3{,}328 cm;$$

$$f_3 = \frac{5}{384} \frac{0.7ql^4}{b_i W_c d} + \frac{l^2}{8} \frac{a}{b_i d} = 2{,}843 cm;$$

$$f_4 = \frac{5}{384} \frac{0.6ql^4}{b_i W_c d} + \frac{l^2}{8} \frac{a}{b_i d} = 2{,}355 cm.$$

The deflections determined by an iteration method based on a non-linear deformation model have the following meanings $f_1 = 3{,}828 cm$ (Δ=0,39%), $f_2 = 3{,}469 cm$ (Δ=4.07 %); $f_4 = 3{,}117 cm$ (Δ=8.79%), $f_4 = 2{,}771 cm$ (Δ=15.01%).

## 6. Conclusion

Methods for calculating hollow triangular cross-section precast-monolithic beams of, as combined structures consisting of two materials with different characteristics, are proposed. In this case, in all methods of calculating cross section rigidity and strength, the hypothesis of flat cross sections is used. Comparative calculations of the strength and stiffness hollow triangular cross section beams showed satisfactory convergence of engineering and iterative methods for their calculation.
In future, it is planned to develop a methodology for hollow triangular section precast-monolithic beams inclined sections calculating.

## References

[1] Azizov, T., Azizova, A., & Al Ghadban, S. (2018). Construction and calculation of reinforced concrete overlap with a high spatial work effect. *International Journal of Engineering and Technology(UAE), 7*(3), 567-574. http://dx.doi.org/10.14419/ijet.v7i3.2.14591

[2] Azizov T.N. Raschet zhelezobetonnyih perekryitiy i prolet-nyih stroeniy mostov / T.N. Azizov, A.Ya. Barashikov, V.S. Dorofeev. - Odessa, 2009. – 193p.

[3] ENV 1992-1. *Eurokode- 2. Design of concrete structure. Part 1, General rules and rules for buildings*, GEN, 1993.

[4] DBN V.2.6-98:2009. *Konstruktsiyi budynkiv i sporud. Betonni ta zalizobetonni konstruktsiyi. Osnovni polozhennya.*, Minrehionbud, Kyiv

[5] Li, G., Wang, B., & Zhou, M. (2018). *Study on Flexural Properties of Reinforced Spontaneous Combustion Gangue Concrete Beams.* Periodica Polytechnica Civil Engineering, 62(1), 206-218. https://doi.org/10.3311/PPci.10647

[6] J. K. Wight, J.G MacGregor . Reinforced Concrete: mechanics and design, New Jersey: Upper Saddle River, (2009).

[7] Rombach G.A. Finite-element Design of Concrete Structures: Practical problems and their solutions, Second edition. ICE Publishing. 2011. - 350p.

[8] Kochkarev, D., & Galinska, T. (2018). Nonlinear Calculations of the Strength of Cross-sections of Bending Reinforced Concrete Elements and Their Practical Realization. Cement Based Materials, 13-30 http://dx.doi.org/10.5772/intechopen.75122

[9] Kochkarev, D., & Galinska, T. (2017). Calculation methodology of reinforced concrete elements based on calculated resistance of reinforced concrete. Paper presented at the *MATEC Web of Conferences, 116* https://doi.org/10.1051/matecconf/201711602020

[10] Kochkarev, D., Galinska, T., & Tkachuk, O. (2018). Normal sections calculation of bending reinforced concrete and fiber concrete element. *International Journal of Engineering and Technology(UAE), 7*(3), 176-182. http://dx.doi.org/10.14419/ijet.v7i3.2.14399

[11] Rzhanitsyin A.R. Teoriya sostavnyih sterzhney stroitelnyih konstruktsiy, Gosstroyizdat. Moskva. 1948, 192

[12] Opir materialiv / G.S. Pisarenko, O.L. Kvitka, E.S. Umanskiy; Za red. G.S. Pisarenko, K.Vyscha shk., 2004, 655.

[13] Storozhenko, L., Butsky, V., & Taranovsky, O. (1998). Stability of compressed steel concrete composite tubular columns with centri-

fuged cores. Journal of Constructional Steel Research, 46(1-3), 484. http://dx.doi.org/10.1016/S0143-974X(98)80098-9
[14] Kochkarev, D., Azizov T., & Galinska, T. (2018) Bending deflection reinforced concrete elements determination. Paper presented at the MATEC Web of Conferences, 230 https://doi.org/10.1051/matecconf/201823002012
[15] Piskunov, V. G., Gorik, A. V., & Cherednikov, V. N. (2000). Modeling of transverse shears of piecewise homogeneous composite bars using an iterative process with account of tangential loads 2. resolving equations and results. Mechanics of Composite Materials, 36(6), 445-452. https://doi.org/10.1023/A:1006798314569
[16] Piskunov, V. G., Goryk, A. V., & Cherednikov, V. N. (2000). Modeling of transverse shears of piecewise homogeneous composite bars using an iterative process with account of tangential loads. 1. construction of a model.Mechanics of Composite Materials, 36(4), 287-296. doi:10.1007/BF02262807